Journal of Thermal Analysis and Calorimetry, Vol. 92 (2008) 2, 403–406

HEAT CAPACITY MEASUREMENT AND DSC STUDY OF HAFNIUM HYDRIDES

Y, Arita[1*], *T. Ogawa*[2], *B. Tsuchiya*[3] *and T. Matsui*[1,2]

[1]Nagoya University, EcoTopia Science Institute, Aichi 464-8603, Japan
[2]Nagoya University, Department of Engineering, Aichi 464-8603, Japan
[3]Tohoku University, Institute for Materials Research, Miyagi 980-8577, Japan

Heat capacities, electrical conductivities and phase transition temperature of hafnium hydrides, HfH_x ($0.99 \le x \le 1.83$), were studied using a direct heating pulse calorimeter and a differential scanning calorimeter from room temperature to above 500 K. The heat capacity of $HfH_{1.83}$ was larger than that of pure hafnium and showed no anomaly of heat capacity. In contrast, there were λ-type peaks for the heat capacity and DSC curves for HfH_x ($1.1 \le x \le 1.6$) near 385 and 356 K. The anomalies of heat capacity and electrical conductivity of HfH_x ($1.1 \le x \le 1.6$) were considered the result of phase transition and order-disorder phase transition for hydrogen in the hafnium hydride lattice for HfH_x ($1.1 \le x \le 1.3$).

Keywords: *electrical conductivity, hafnium hydride, heat capacity, phase transition*

Introduction

The group IV transition metals, titanium, zirconium and hafnium, are excellent materials for aerospace, nuclear reactors and biocompatible objects because of their high corrosion resistance due to their good passivation with an oxide scale. Hafnium has a significant neutron absorption capacity and capture cross section with regard to thermal neutrons, and does not generate certain gases, such as helium, that are absorbed by boron carbide control rods during a nuclear reaction. Hafnium also stores many hydrogen atoms. Since the density of hydrogen atoms in hafnium hydrides (HfH_x) is comparable to that in liquid hydrogen, hafnium hydrides can also be used as fast neutron moderators to gain thermal neutrons. Therefore, HfH_x was proposed as control rods for fast neutron flux process in fast reactors [1]. In order to design control rods using HfH_x, thermophysical properties and phase relations of the hydrides are important. However, the study of thermal properties of HfH_x has been limited for the thermal diffusivity [2].

In this study, heat capacities and electrical conductivities for HfH_x ($1.1 \le x \le 1.6$) were measured and the phase transition behaviors of HfH_x ($0.99 \le x \le 1.83$) were investigated with differential scanning calorimetry.

Experimental

Sample preparation

Samples of HfH_x were prepared by heating rod and sheet samples of pure hafnium metal (Nilaco, 99.9% quality; including <3% niobium) at 1173 K, followed by exposure to 99.9% pure hydrogen gas flow at 973, 1073, 1123 and 1173 K for 6, 4 and 2 h, respectively. The rod sample annealed at 973 K was blistered and cracked from storing hydrogen. The prepared samples were found to consist of mixtures of α-phase and δ (δ')-phase from X-ray diffraction analysis. The compositions of the specimens were calculated based on the mass change after de-hydrogenations. The details of the samples are tabulated in Table 1.

Measurements of heat capacity, electrical conductivity and DSC curve

The heat capacity and the electrical conductivity were simultaneously measured from room temperature to 500~600 K, to avoid dehydration, for HfH_x (x=1.11, 1.47 and 1.83) and to 950 K for pure Hf by a direct heating pulse calorimeter, for which the details have been given elsewhere previously [3, 4]. The samples for heat capacity and electrical conductivity measurements were 2 mm in diameter and 30 mm in length. Differential scanning calorimetry (DSC) curves were observed for each composition from room temperature to 473 K in an argon atmosphere with heating rates of 5, 10 and 20 K min^{-1}. The powdered samples were prepared by pulverizing part of the rod samples in this study and a previous study [2] for DSC measurements. Phase transition temperatures were evaluated by extrapolating the onset temperatures to a zero heating rate. The enthalpy of the phase transition was also evaluated from the DSC curve using the heat of

* Author for correspondence: arita@esi.nagoya-u.ac.jp

1388–6150/$20.00

Akadémiai Kiadó, Budapest, Hungary
Springer, Dordrecht, The Netherlands

Table 1 Samples for measurements

H/Hf	Anneal temp./K	Phase	Transition temp./K	ΔH_{exp}/ kJ mol^{-1}	ΔS_{exp}/ J mol^{-1} K^{-1}	ΔS_{cal}/ J mol^{-1} K^{-1}
1.83	[2]	ε	–	–	–	–
1.60	973	δ’	388.9	2.14	5.5	–
1.47	1073	α+δ’	386.7	1.93	5.0	–
1.30	1123	α+δ’ (+γ)	380.6, 356.7	1.04*	2.8	10.8
1.11	1173	α+δ’(+γ)	356.4	1.84	5.2	11.4
0.995	[2]	α+δ’(+γ)	–	–	–	–

*total area including two peaks

fusion for pure indium. The melting point of indium is 429.75 K and it is used as the standard.

Results and discussion

The results of the heat capacity measurements on $HfH_{1.11}$ and $HfH_{1.47}$ are shown in Fig. 1, and those of $HfH_{1.83}$ and pure Hf are shown in Fig. 2. As seen in Fig. 1, a λ-type heat capacity anomaly was observed for each sample. However there was no anomaly for the heat capacity for $HfH_{1.83}$ and pure Hf. The electrical conductivities of HfH_x (x=1.11, 1.47 and 1.83) and Hf are shown in Fig. 3. The electrical conductivities of $HfH_{1.11}$ and $HfH_{1.47}$ showed a jump at the temperature corresponding to the heat capacity anomaly. The value and temperature dependence of the electrical conductivities below the phase transition temperature were almost the same as each other. The electrical conductivities for $HfH_{1.83}$ and pure Hf decreased monotonically with increasing temperature. The electrical conductivities of HfH_x, x=1.11, 1.47 and 1.83, showed similar values above 400 K.

The DSC curves of HfH_x (x=0.995, 1.11, 1.30, 1.47 and 1.60) are shown in Fig. 4. A peak corresponding to a phase transition was seen in the DSC curve for $HfH_{1.11}$, $HfH_{1.47}$ and $HfH_{1.60}$. However there were two peaks in the DSC curve for $HfH_{1.30}$. The phase transition temperatures were estimated by analyzing an onset temperature in the DSC curve. Estimated transition temperatures are tabulated in Table 1 and showed in Fig. 5 with the phase diagram [5]. The

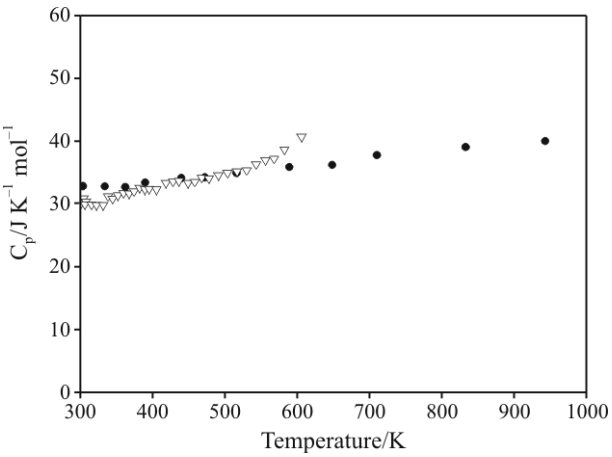

Fig. 2 Heat capacity of $HfH_{1.83}$ and Hf; ▽ – $HfH_{1.83}$, and ● – Hf

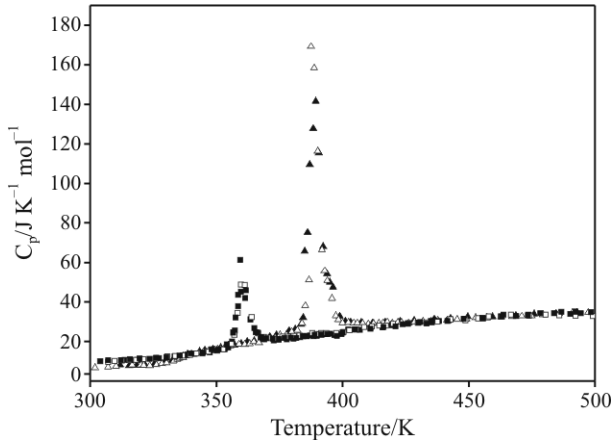

Fig. 1 Heat capacity; ▲ – $HfH_{1.47}$ 1st run, △ – $HfH_{1.47}$ 2nd run, □ – $HfH_{1.11}$ 1st run and ■ – $HfH_{1.11}$ 2nd run

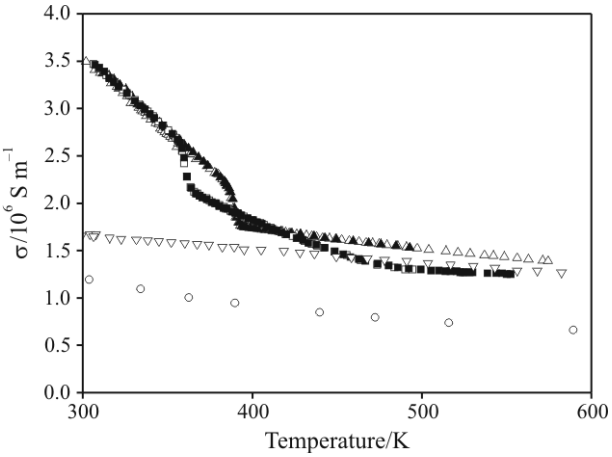

Fig. 3 Electrical conductivity of HfH_x; ▲ – $HfH_{1.47}$ 1st run, △ – $HfH_{1.47}$ 2nd run, □ – $HfH_{1.11}$ 1st run, ■ – $HfH_{1.11}$ 2nd run, ▽ – $HfH_{1.83}$, ❍ – Hf

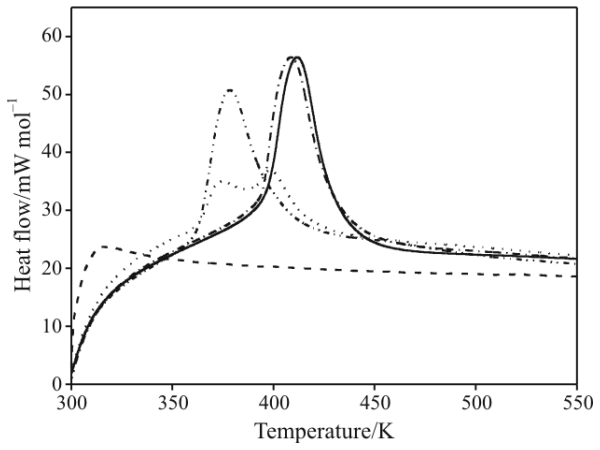

Fig. 4 DSC signals for HfH_x; — – $HfH_{1.60}$, –·– – $HfH_{1.47}$, ··· – $HfH_{1.30}$, –··– – $HfH_{1.11}$, --- – $HfH_{0.995}$

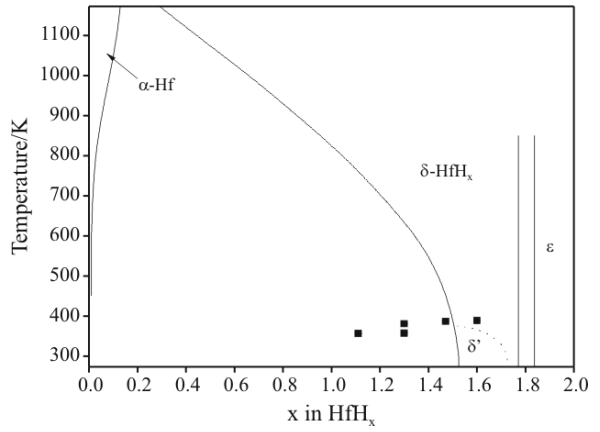

Fig. 5 Phase diagram of HfH_x proposed by Massalski *et al.* [5] and transition temperature observed in this study

temperatures of δ'- to δ-phase transition observed in this study were higher than that in the previous phase diagram and the phase boundary should extend to the α+δ region in the phase diagram.

In the hafnium-hydrogen system, a small amount of hydrogen could solute into the hexagonal α-Hf. The crystal structures of the compositions with $1.72 \le x \le 1.77$ and $1.83 \le x \le 2.02$ were face-centered cubic δ-phase and face-centered tetragonal (body-centered tetragonal) ε-phase, respectively [6–8]. The crystal structure of the composition with $1.53 \le x \le 1.72$ exhibited a pseudo-cubic defect δ-phase (δ'phase) [8–10]. The unit cell of this pseudo-cubic phase is slightly deformed and displays some tetragonal characteristics, such as the lattice constants for the *a* and *b*-axes having the same values as those of the δphase, while that for the *c*-axes is lower. It was also confirmed from diffraction patterns obtained from TEM observation experiments during annealing to 673 K that the deformed cubic phase converts into a face-centered cubic phase at temperatures above 353 K [2]. The phase transition at 380~390 K should correspond to the δ'–δ transition. Meanwhile, the origin of the transition at 356 K was not clear.

The hydrogen atoms in the ε-phase and δ-phase are located in vacant tetrahedral interstices [5]. In zirconium–hydrogen and titanium–hydrogen system, the existence of γ-phase, which is the tetragonal and ordered-hydrogen structure, were indicated [11, 12]. The proposed crystal structure of γ-phase was that hydrogen atoms are alternately located at the tetrahedral site on 220 planes in a fct (Face centered tetragonal) δ'-phase and the stoichiometric chemical composition, H/Ti(Zr), is unity. In the hafnium–hydrogen system, it was also suggested that a similar crystal structure exists around H/Hf=1. The crystal lattice structure of ε-HfH_2 is similar to a CaF_2 type structure. As the concentration of hydrogen decreases, hydrogen vacant sites may be created randomly in the HfH_2 lattice (disordered phase), and the alignment of the hydrogen atom in HfH_1 is considered to alternate (ordered phase). The anomaly of the heat capacity and DSC curve observed at 356 K for hydrogen dissolved HfH_x (x=1.11 and 1.30) in this study was thought to be due to an order-disorder rearrangement of hydrogen atoms.

The entropy change assumed to be due to the order–disorder transition can be calculated theoretically as follows. The hydrogen atoms are distributed in tetrahedral sites in a bct (body centered tetragonal) metal subcell. Since hydrogen atoms occupy hydrogen sites randomly in the high temperature (disordered) phase, the number of available hydrogen sites is double the number of metal atoms N and the entropy change ΔS is calculated as follows, assuming a perfect ordering in the low-temperature phase,

$$\begin{aligned}\Delta S &= k\ln\frac{2N!}{xN!(2N-xN)!} \\ &= -R\{x\ln x+(2-x)\ln(2-x)-2\ln 2\}\end{aligned} \quad (1)$$

where N and x are the number of metal sites and the H/Hf ratio, respectively. The calculated ΔS_{cal} values are given in Table 1.

The present results of transition enthalpy and entropy change at the transitions are also summarized in Table 1. Although ΔS_{cal} values of $HfH_{1.30}$ and $HfH_{1.11}$ were larger than the ΔS_{exp} values, the ΔS_{cal} values will be smaller considering the amounts of γ-phase after decision of phase boundary.

Since the phase diagram of hafnium–hydrogen [5] has not been completely established, the origin of the phase transition is not yet clear. The mechanism of the phase transition should be clarified by more detailed studies such as neutron diffraction or analysis of the vibration spectrum. However, it was shown that the temperature of the δ'- to δ-phase tran-

sition should be higher than that of the previous phase diagram, there is an α+δ' region in the phase diagram and a hydrogen-ordered phase around 1≤H/Hf≤1.3.

Conclusions

A λ-type peak corresponding to a phase transition was observed in the heat capacity of HfH_x (x=1.11 and 1.47). There was also a peak in the DSC curves for HfH_x (x=1.11, 1.30, 1.47 and 1.60). There were two peaks in the DSC curve for $HfH_{1.30}$. The transition temperatures estimated from heat capacity measurements and DSC measurements were 380~390 K and about 356 K. For H/Hf≥1.3, the anomalous peak around 380~390 K were considered to originate from a phase transition from the δ'- to δ-phase, whereas for 1≤H/Hf≤1.3, the anomalous peak around 356 K was considered to be the result of an order–disorder transition of hydrogen atoms.

Acknowledgements

This work was partly supported by Grant-in-Aid for Scientific Research (C), No. 17560596, 2005–2006.

References

1 K. Konashi, T. Iwasaki, T. Terai, M. Yamawaki, K. Kurosaki and K. Itoh, Proc. ICAPP'06, Reno, USA 2006.
2 B. Tsuchiya, M. Teshigawara, K. Konashi, S. Nagata and T. Shikama, J. Alloys Compd., 446-447 (2007) 439.
3 K. Naito, H. Inaba, M. Ishida and K. Seta, J. Phys. E, 12 (1979) 712.
4 Y. Arita, K. Suzuki and T. Matsui, J. Phys. Chem. Solids, 66 (2005) 231.
5 T. B. Massalski, Binary Alloy Phase Diagrams 2nd Ed., ASM International, Materials Park, Ohio 1990.
6 S. S. Sidhu, Acta Cryst., 7 (1954) 447.
7 S. S. Sidhu, L. Heaton and D. D. Zauberis, Acta Cryst., 9 (1956) 607.
8 S. S. Sidhu and J. C. McGuire, J. Appl. Phys., 23 (1952) 1257.
9 L. Espagno, P. Azou and P. Bastien, Compt. Rend., 250 (1960) 4352.
10 R. K. Edwards and E. Veleckis, J. Phys. Chem., 66 (1962) 1657.
11 H. Numakura and M. Koiwa, Acta Metall., 32 (1984) 1799.
12 R. L. Beck, Trans. ASM, 55 (1962) 542.
13 S. S. Sidhu, N. S. Satya Murthy, F. P. Campos and D. D. Zauberis, Adv. Chem. Ser., 39 (1963) 87.
14 H. Numakura, M. Koiwa, H. Asano and F. Izumi, Acta Metall., 36 (1988) 2267.

DOI: 10.1007/s10973-007-8960-4